

Supplement of Atmos. Chem. Phys., 18, 17143–17155, 2018
<https://doi.org/10.5194/acp-18-17143-2018-supplement>
© Author(s) 2018. This work is distributed under
the Creative Commons Attribution 4.0 License.



Atmospheric
Chemistry
and Physics
Open Access


Supplement of

The influence of particle composition upon the evolution of urban ultrafine diesel particles on the neighbourhood scale

Irina Nikolova et al.

Correspondence to: A. Rob MacKenzie (a.r.mackenzie@bham.ac.uk)

The copyright of individual parts of the supplement might differ from the CC BY 4.0 License.

13 Here we present details of the input parameters used in the box model simulations (Section S1) and
14 some results (Section S2). All figures and tables are given in the Appendix.

15

16 **S1. Model input parameters** - size distribution, vapour pressures, modal composition mass
17 fractions in the nucleation and Aitken modes, gas-phase ambient concentrations.

18

19 The initial size distribution is based on the measurements of Dall'Osto et al. (2011) and it is plotted
20 in Figure 1-S. This ultrafine size resolved distribution represents the typical street canyon size
21 distribution found next to a traffic site in Marylebone road in London (UK). The distribution has a
22 well defined nucleation mode (particles with a diameter around or less than 30 nm) with a peak
23 number concentration at ~ 23 - 24 nm. The Aitken mode (particles with diameter between 30 and
24 100 nm) is seen as a shoulder attached to the nucleation mode with a centre between 50 - 60 nm.
25 Dall'Osto et al. (2011) show that the observed size distribution is subject to a major transformation
26 caused by extensive evaporation of volatile material from the particles. The diameter of the
27 nucleation mode particles decreased during the transport of the particles between the street canyon
28 and the nearby city park over a distance of about 665m, as shown in Figure 1-S in the Appendix.

29 The nucleation-mode peak diameter, $D_{pg,nuc}$, corresponding to the highest number concentration in
30 the nucleation mode, was found at around 8 – 9 nm. In our study, we aim to put forward a realistic
31 set of compositions and thermodynamic properties that could explain this diameter decrease as seen
32 in the observations. Chemical analyses during the observations are missing; however, there are
33 some laboratory data pointing to the nature of organics that participate in the composition from
34 emitted particles collected from an engine testbed (Alam et al., 2016). Figure 2-S shows the
35 normalised mass concentration per compound in the range $[C_{16}H_{34}:C_{32}H_{66}]$ for a given size class.
36 Particles in the Nucleation and Aitken modes consist of about 10% and higher contribution from
37 compounds in the range $C_{25}H_{52}-C_{29}H_{60}$.

38

$$M_{ij} = \sum_{k=1}^2 \frac{\pi}{6} Dp_i^3 \rho X_{jk} N_{ik}$$

39 In our modelling study the UFP size-resolved mass composition per mode (eq. 1) is initialised as
 40 follows. The mass of a particle, M_{ij} , per size bin i and compound j in the range [C₁₆H₃₄:C₃₂H₆₆] is
 41 expressed as

(eq. 1)

42 $i = 1, \dots, 15$ – number of size bins

43 $j = 1, \dots, 18$ – indices [1-17] correspond to surrogate n-alkane compounds in the range C₁₆H₃₄ –
 44 C₃₂H₆₆; index 18 refers to the involatile core

45 $k = 1, 2$ - particle mode, where 1 = Nucleation mode, 2 = Aitken mode

46 Dp_i – particle diameter per size bin i , m

47 M_{ij} – size resolved mass per size bin i and per compound j , kg m⁻³

48 $\rho = 1000$ kg m⁻³, particle density, held constant to avoid introducing highly uncertain parameters for
 49 density of involatile core.

50 X_{jk} – fraction of mass in a particle in mode k per compound j

51 $\pi = 3.14$

52 and

$$N_{ik} = n(Dp)_{ik} \Delta Dp$$

53 in which $n(Dp)$ is the differential size distribution and N_{ik} is the number of particles per bin width
 54 ΔDp , [$\# \text{ m}^{-3}$]. The number log-normal size distribution (eq. 2) is given as follows:

55

$$n(Dp)_{ik} = \frac{N_k}{\sqrt{(2\pi)} Dp_i \ln(\sigma_{gk})} \exp\left(-0.5 \left(\frac{\ln(Dp_i / Dp_{gk})}{\ln(\sigma_{gk})} \right)^2\right)$$

56

(eq. 2)

57

58

59 $N_k = 3.0 \times 10^{10}$ and 1.8×10^{10} ($\# \text{ m}^{-3}$) are the total number concentrations in the Nucleation and Aitken
 60 mode, respectively

61 $Dp_{gk} = 23$ and 65 nm are the geometric mean diameter in the Nucleation and Aitken mode,

62 respectively

63 $\sigma_{gk} = 1.6$ is the geometric standard deviation for both modes

64 The fraction of mass X_{jk} of each particle in a mode k per compound SVOC in the range C₁₆H₃₄-

65 C₃₂H₆₆ is calculated (eq. 3) as follows:

$$X_{jk} = \frac{f(x_j | m_j, \sigma_{modal})}{\sum_{j=1}^{17} f(x_j | m_j, \sigma_{modal})} (x x_{jk} - s f_k)$$

66 (eq. 3)

67 where $f(x_j | m_j, \sigma_{modal})$ is the modal composition in the form of a Gaussian distribution (eq. 4), $x x_{jk}$ is

68 SVOC composition given by the Gaussian parameterisation (eq. 5), and $s f_k$ is the solid involatile

69 fraction per mode k :

70

$$f(x_j | m_j, \sigma_{modal}) = \frac{1}{\sqrt{(2\pi)\sigma_{modal}}} \exp\left(-0.5\left(\frac{(x_j - m_j)}{\sigma_{modal}}\right)^2\right)$$

71 (eq. 4)

72

$$x x_{jk} = \sum_{j=1}^{17} \frac{f(x_j | m_j, \sigma_{modal})}{\sum_{j=1}^{17} f(x_j | m_j, \sigma_{modal})} = 1$$

73 (eq. 5)

74

75 $\sigma_{modal} = 1, \dots, 5$ – standard deviation of modal composition

76 $x_j = 1, \dots, 17$ – number assigned to the SVOC compound

77 $m_j = 1, \dots, 17$ – modal composition compound for each SVOC in the range C₁₆H₃₄-C₃₂H₆₆

78

79 In this study the role of an involatile core ($s f_k$) is evaluated, too, by considering an involatile core to

80 be 1%, 5% and 10% of the mass in a particle in the Nucleation mode ($k = 1$). Input modal

81 composition mass fractions in the nucleation mode and composition standard deviation are
82 presented in the Appendix in Table 1-S, 2-S and 3-S for involatile core of 1%, 5% and 10%,
83 respectively. The involatile core in the Aitken mode is 90% and the input modal composition mass
84 fractions are given in Table 4-S in the Appendix.

85

86 Input vapour pressure parameterisations are given in Table 5-S. A-a, B-c and Co are used in this
87 study to represent the uncertainties in the vapour pressure and evaluate the overall effect on the
88 evaporative shrinkage of the nucleation mode particle diameter. Figure 3-S shows the ratio of
89 vapour pressure between 298 K and 273 K for A-a, B-c and Co vapour pressure parameterisations
90 and n-alkane compounds in the range $C_{16}H_{34}$ - $C_{32}H_{66}$. The ratio for B-c and Co vapour pressure
91 parameterisations is within an order of magnitude for compounds in the range $C_{16}H_{34}$ - $C_{25}H_{52}$,
92 however, it increases two to three orders of magnitude for higher molecular weight compounds. The
93 ratio for A-a vapour pressure parameterisation is within an order of magnitude for compounds in the
94 range $C_{16}H_{34}$ - $C_{21}H_{44}$, and increases substantially for the remaining compounds. This would imply
95 that for the selected timescale of 100 s there will be a shift in the threshold modal compositions to
96 lower carbon-number compounds in comparison with the threshold modal compositions discussed
97 in this study. The temperature dependence on evaporation is not considered further in this study but
98 should be borne in mind. The effect of changing the mass accommodation coefficient is discussed in
99 section 3.4 of the main text.

100

101 The initial gas-phase concentrations for the n-alkanes in the range $C_{16}H_{34}$ - $C_{32}H_{66}$ (Table 6-S) are as
102 for the study in Nikolova et al. (2016) and are based on the roadside atmospheric measurements of
103 Harrad et al. (2003).

104

105 **S2. Results**

106 Figure 4-S and Figure 5-S show the nucleation mode peak diameter $D_{pg,nuc}$ after 100 s using the

107 vapour pressure parameterisations following Myrdal-Yalkowsky et al (1997, B-c) and Nannoolal et
108 al (2008, A-a), respectively. The nucleation mode particles consist of initial 1% non-volatile
109 material. The threshold modal composition value changes from C₂₇H₅₆ for the B-c parameterisation
110 (Figure 4-S) to C₂₂H₄₆ for A-a (Figure 5-S).

111

112 Figure 6-S shows the relative difference of the D_{pg,nuc} between the highest (B-c) and lowest (A-a)
113 vapour pressure parameterisations evaluated at 1 s, 10 s, 50 s and 100 s. Overall the largest
114 difference is propagating to higher standard deviation sigma when simulation time increases as well
115 as moving towards higher carbon-number modal compositions. In other words the relative
116 differences become larger with time, pointing back to the huge differences in vapour pressure
117 parameterisations between B-C and A-a. The choice of a particular vapour pressure dataset changes
118 the range of carbon numbers by 2 in the first 10 seconds for which the highest relative difference is
119 simulated. The 1-s relative difference is the highest for sigma 1 and modal compositions C₁₉H₄₀-
120 C₂₁H₄₄. The 10-s highest relative difference has shifted to modal compositions C₂₁H₄₄-C₂₃H₄₈ and
121 sigma = 1, 2. Higher relative differences (50% and more) are also simulated at sigma = 3. The 100-s
122 relative difference is the highest for modal compositions C₂₂H₄₆-C₂₄H₅₀ and sigma = 1, 2, 3, but also
123 relative differences of around 50% are simulated for sigma = 5.

124

125 Figure 7-S shows the ‘100-s effective involatile core’ for the nucleation mode particles. Results are
126 shown at 1%, 5% and 10% initial non-volatile material in the nucleation mode particles, modal
127 compositions C₂₄H₃₄ and C₃₂H₆₆ and for various composition standard deviations, sigma. Vapour
128 pressure parameterisations follow Myrdal and Yalkowski (1997; B-c in Table 1-S) and Nannoolal et
129 al. (2008; A-a in Table 1-S). Figure 5-S presents the sensitivity to the non-volatile core in the
130 nucleation mode for modal compositions C₂₄H₅₀ and C₃₂H₆₆ evaluated for B-c and A-a vapour
131 pressure parameterisations. The 100-s effective involatile core for modal composition C₂₄H₅₀ and B-
132 c vapour pressure parameterisation increases when the non-volatile core increases. This is simulated

133 for an increasing σ too, due the increasing number of lower volatility components that are added
134 into the particle composition. The 100-s effective involatile core for modal compositions C₂₄H₅₀ (for
135 A-a vapour pressure) and C₃₂H₆₆ (for A-a and B-c vapour pressures) shows an opposite trend with
136 respect to sigma, i.e., the 100-s effective involatile core decreases due to the increasing number of
137 higher volatility components added into the particle composition.

138

139 Figure 8-S shows the nucleation mode peak diameter D_{pg,nuc} after 100 s for different values of the
140 mass accommodation coefficient (α), modal composition, and composition standard deviation (σ),
141 using the vapour pressure parameterisations following Myrdal-Yalkowsky et al (1997, B-c) and
142 Nannoolal et al (2008, A-a), respectively. The nucleation mode particles consist of initial 1% non-
143 volatile material and modal composition C₂₄H₅₀ and C₃₂H₆₆, i.e. less volatile compositions that
144 shown in Figure 8 of the main text. A wide range of D_{pg,nuc} can result from different values of α and
145 σ for a modal composition of C24H50 and the B-c vapour pressure parameterisation (see main text
146 Figure 3 for vapour pressure nomenclature). For the other combinations of modal composition and
147 vapour pressure parameterisation shown, the choice of α has little effect on the model results.

148

149

150 **Acknowledgements**

151 This work is part of the FASTER project, ERC-2012-AdG, Proposal No. 320821 sponsored by the
152 European Research Council (ERC).

153

154 **References**

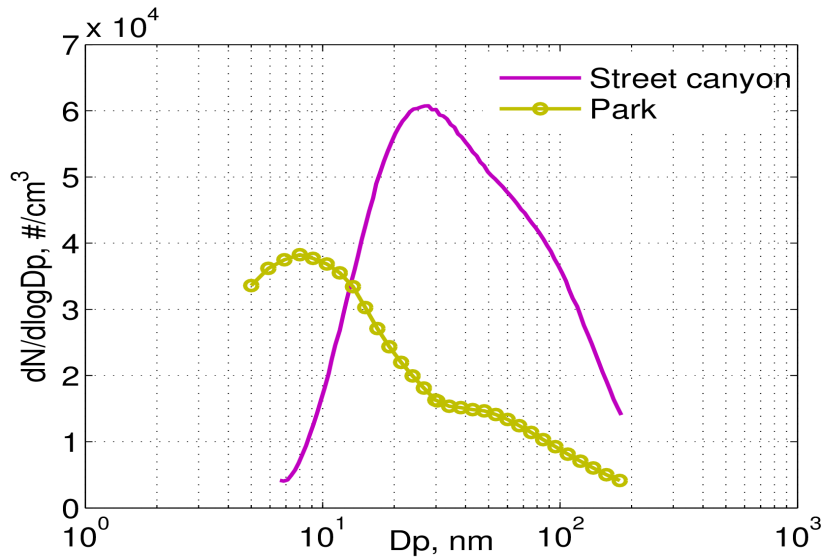
155

156 Alam, M. S, Rezaei, S. Z., Stark, C. P., Liang, Z., Xu, H. M., Harrison, R. M.: The
157 characterisation of diesel exhaust particles – composition, size distribution and partitioning,
158 Faraday Discuss., 189, 69-84, 2016.

159

160 Chickos, J., Lipkind, D.: Hypothetical thermodynamic properties: vapour pressures and
161 vaporization enthalpies of the even n-Alkanes from C78 to C92 at T= 298.15K by correlation-gas
162 chromatography, J. Chem. Eng. Data, 53, 2432-2440, 2008.

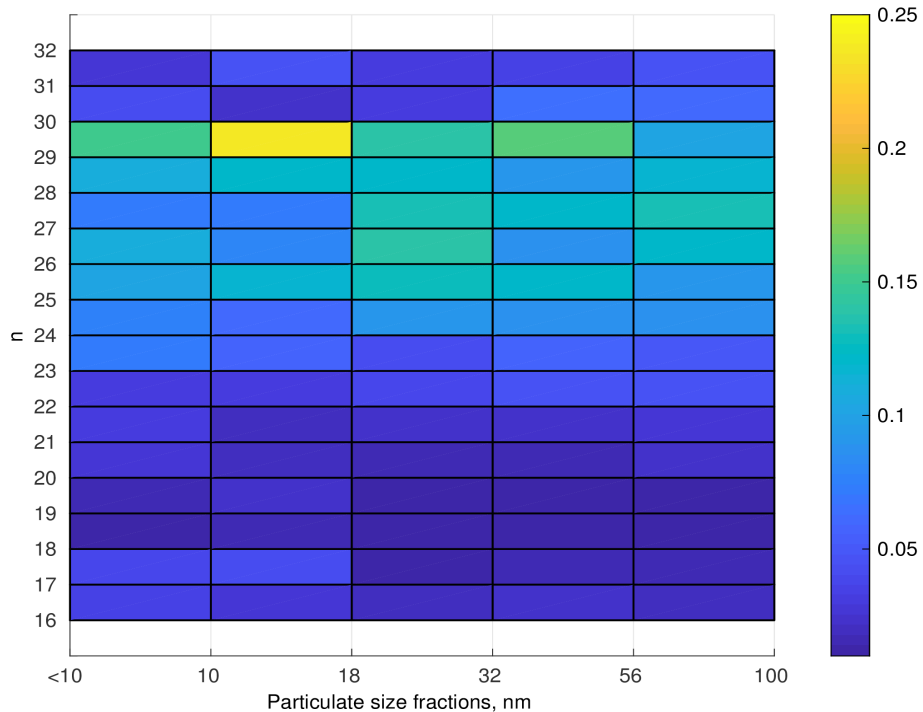
- 163
164 Compernolle, S., Ceulemans, K., Muller, J. -F.: EVAPORATION: a new vapour pressure estimation
165 method for organic molecules including non-additivity and intramolecular interactions, *Atmos.*
166 *Chem. Phys.*, 11, 9431-9450, 2011.
167
168 Dall'Osto, M., Thorpe, A., Beddows, D.C.S., Harrison, R.M., Barlow, J.F., Dunbar, T., Williams,
169 P.I., Coe, H.: Remarkable dynamics of nanoparticles in the urban atmosphere, *Atmos. Chem. Phys.*,
170 11, 6623-6637, 2011.
171
172 Joback, K., Reid, R.: Estimation of pure-component properties from group-contributions, *Chem.*
173 *Eng. Commun.*, 57, 233-243, 1987.
174
175 Harrad, S., Hassoun, S., Callen Romero, M. S., Harrison, R. M.: Characterisation and source
176 attribution of the semi-volatile organic content of atmospheric particles and associate
177 vapour phase in Birmingham, UK , *Atmos. Environ.*, 37, 4985-4991, 2003.
178
179 Myrdal, P. B., Yalkowsky, S. H.: Estimating pure component vapor pressures of complex organic
180 molecules, *Ind. Eng. Chem. Res.*, 36, 2494-2499, 1997.
181
182 Nannooolal, Y., Rarey, J., Ramjugernath, D., Cordes, W.: Estimation of pure component properties:
183 Part 1. Estimation of the normal boiling point of non-electrolyte organic compounds via
184 group contributions and group interactions, *Fluid Phase Equilibr.*, 226, 45-63, 2004.
185
186 Nannooolal, Y., Rarey, J., Ramjugernath, D.: Estimation of pure component properties: Part 3.
187 Estimation of the vapor pressure of non-electrolyte organic compounds via group contributions and
188 group interactions, *Fluid Phase Equilibr.*, 269, 117-133, 2008.
189
190 Nikolova, I., MacKenzie, A. R., Cai, X., Alam, M. S., Harrison, R. M.: Modelling component
191 evaporation and coposition change of traffic-induced ultrafine particles during travel from street
192 canyon to urban background, *Faraday Discuss.*, 189, 529-46, 2016.
193
194 Stein, S. E., Brown, R. L.: Estimation of normal boiling points from group contributions, *J. Chem.*
195 *Inf. Comp. Sci.*, 34, 581-587, 1994.
196
197
198 Topping, D., Barley, M., Bane, M. K., Higham, N., Aumont, B., Dingle, N., McFiggans, G.:
199 UManSysProp v1.0: an online and open-source facility for molecular property prediction and
200 atmospheric aerosol calculations, *Geosci. Model Dev.*, 9, 899-914, 2016.
201
202



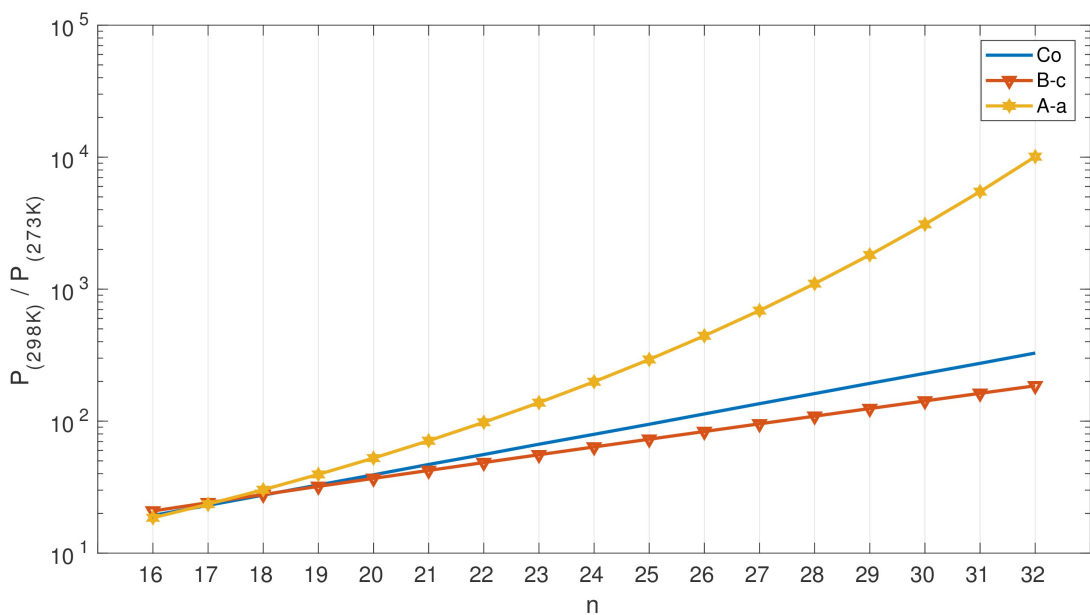
204

205 *Figure 1-S. Measured ultrafine particle size distribution in a street canyon (Marylebone Road,
206 London, UK) and the nearby city park (Regents Park, London, UK).*

207



208 *Figure 2-S. Laboratory particulate mass fractions of n-alkanes $C_nH_{(2n+2)}$, where $n=[16:32]$ for
209 selected particulate diameter range [$<10:100$ nm]. Figure plotted based on the data presented in
210 Alam et al. (2016).*



211 *Figure 3-S. Vapour pressure ratios for vapour pressure parameterisations A-a, B-c and Co and n-*
 212 *alkane compounds $C_nH_{(2n+2)}$, $n=[16:32]$, between 298 K and 273 K.*
 213

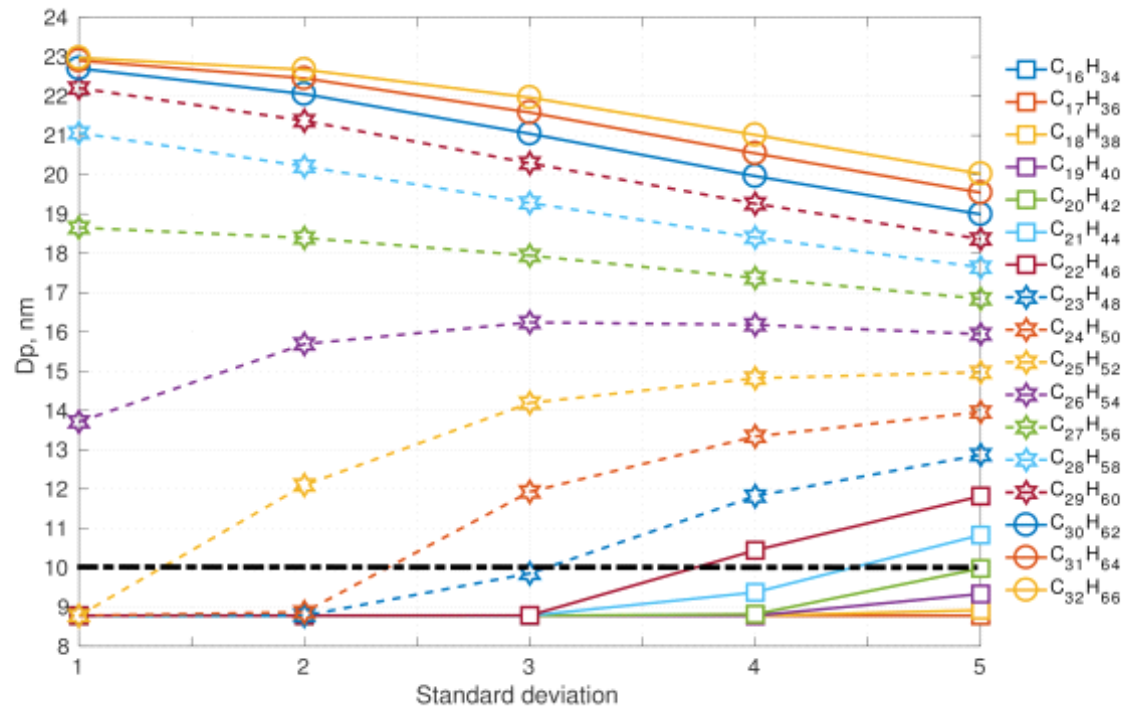


Figure 4-S. Nucleation mode peak diameter D_p [nm] at 100 s of simulation depending on the modal composition and the composition standard deviation. The initial nucleation mode peak diameter is at 23 nm (not shown on the figure). Vapour pressure data follows Myrdal Yalkowsky et al. (1997, B-c). Initial nucleation mode particle involatile core is 1%.

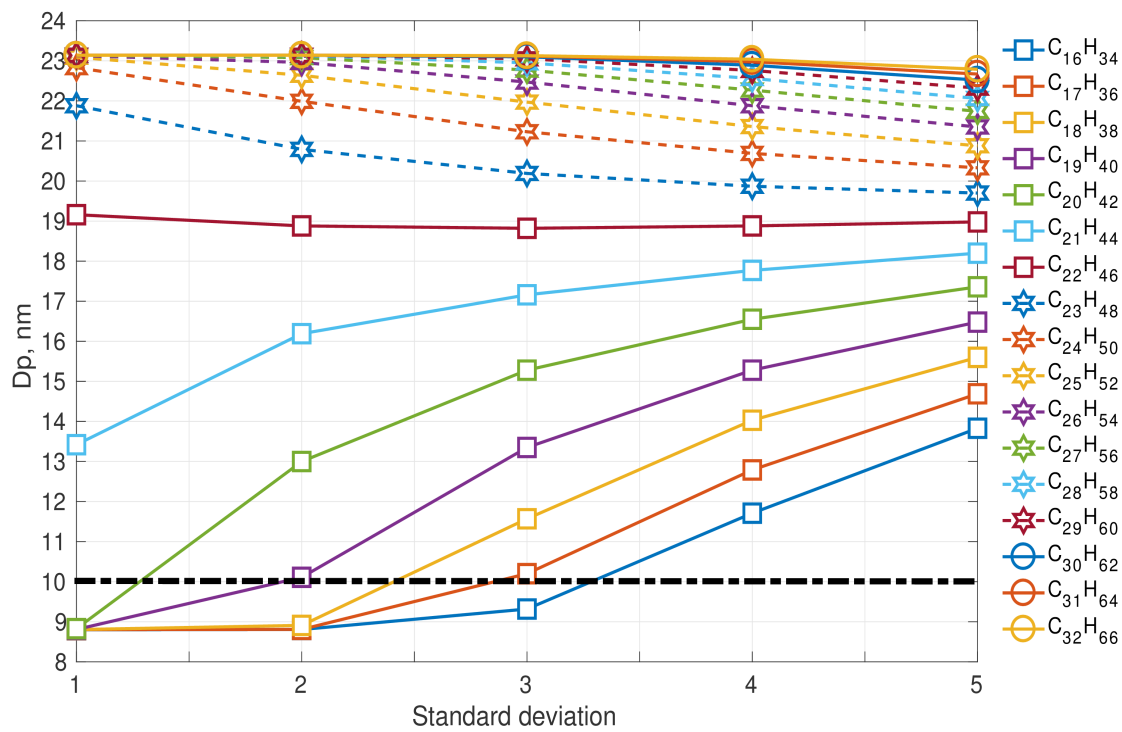
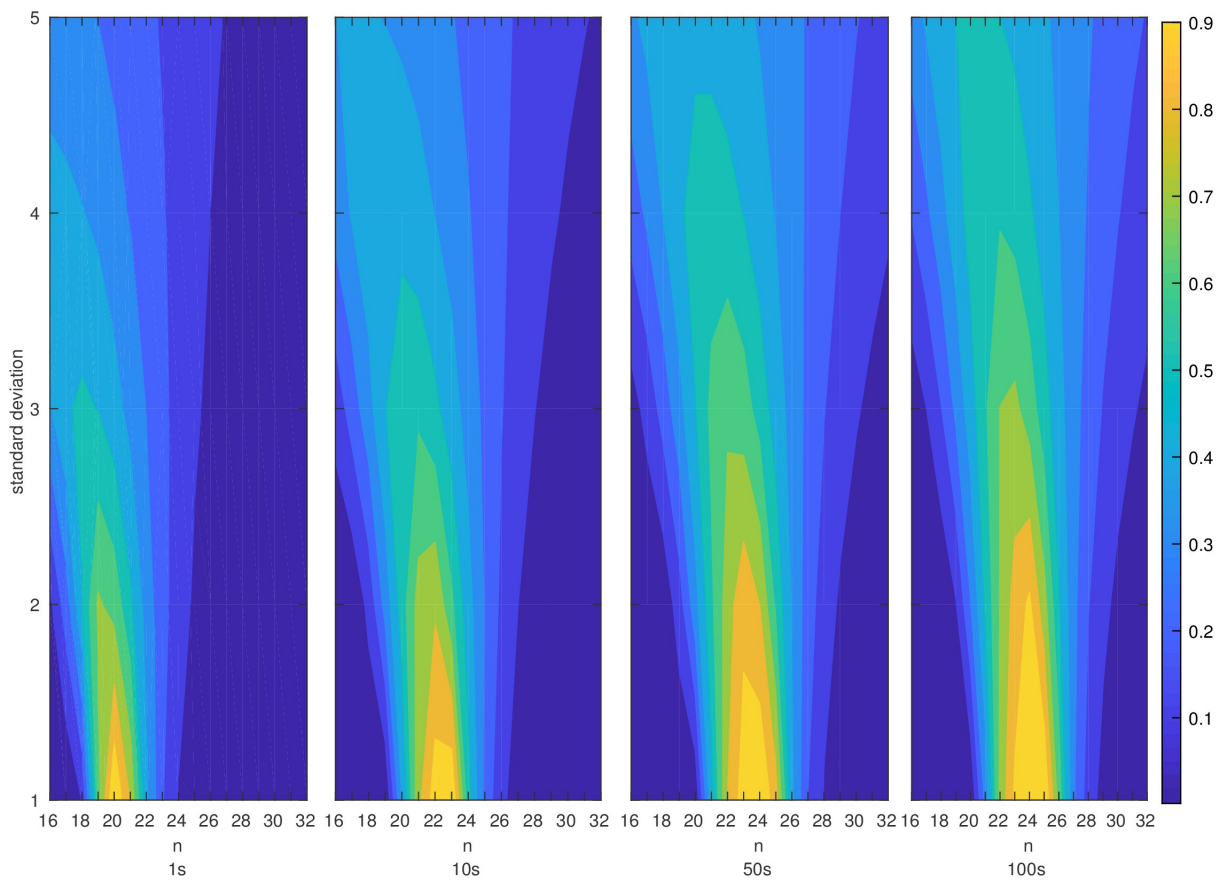


Figure 5-S. Nucleation mode peak diameter Dp [nm] at 100 s of simulation depending on the modal composition and the composition standard deviation. The initial nucleation mode peak diameter is at 23 nm (not shown on the figure). Vapour pressure data follows Nannoolal et al. (2008, A-a). Initial nucleation mode particle involatile core is 1%.



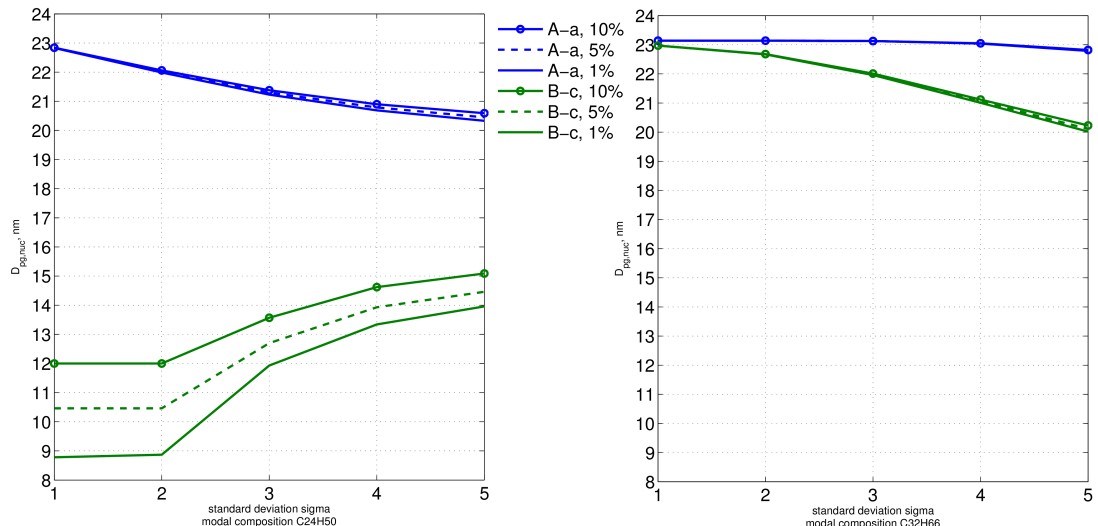
215 *Figure 6-S. Nucleation mode peak diameter relative difference (in %) between B-c and A-a vapour*
 216 *pressure parameterisations for modal compositions $C_nH_{(2n+2)}$ for $n = 16:32$ and composition*
 217 *standard deviation from 1 to 5.*

218

219

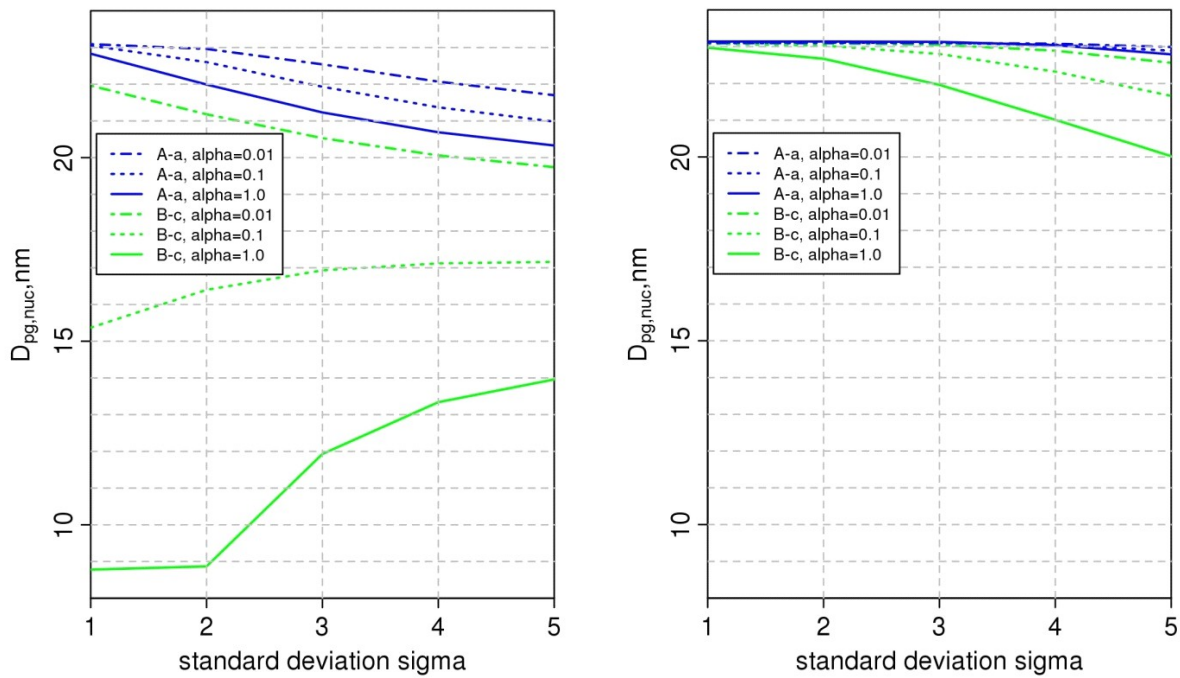
220

221



222 *Figure 7-S. Nucleation mode peak diameter D_p [nm] after 100s: the ‘100-s effective involatile core’*
223 *for the nucleation mode. Results are shown at 1%, 5% and 10% initial non-volatile material in the*
224 *nucleation mode particles, modal compositions $C_{24}H_{50}$ (left) and $C_{32}H_{66}$ (right) and for various*
225 *composition standard deviations, sigma. Vapour pressure parameterisation follows Myrdal and*
226 *Yalkowski (1997; B-c in Table 1-S) and Nannoolal et al. (2008; A-a in Table 1-S).*

227



229 *Figure 8-S. Nucleation mode peak diameter D_p [nm] at 100 s of simulation depending on the mass*
 230 *accommodation coefficient, the vapour pressure parameterisation, and the composition standard*
 231 *deviation. Results are shown at accommodation coefficients of 0.01, 0.1 and 1.0, modal*
 232 *compositions $C_{24}H_{50}$ (left) and $C_{32}H_{66}$ (right) and for various composition standard deviations,*
 233 *sigma. Vapour pressure parameterisation follows Myrdal and Yalkowski (1997; B-c in Table 1-S)*
 234 *and Nannoolal et al. (2008; A-a in Table 1-S).*
 235

σ	modal composition																				
1	$C_{10}H_{34}$	C_9H_{38}	C_8H_{46}	C_7H_{50}	C_6H_{52}	C_5H_{44}	C_4H_{46}	C_3H_{48}	$C_{24}H_{50}$	$C_{23}H_{52}$	$C_{22}H_{54}$	$C_{21}H_{56}$	$C_{20}H_{58}$	$C_{19}H_{60}$	$C_{18}H_{62}$	$C_{17}H_{64}$	$C_{16}H_{66}$	$C_{15}H_{68}$	$C_{14}H_{70}$	$C_{13}H_{72}$	$C_{12}H_{74}$
2	$C_{10}H_{34}$	C_9H_{38}	C_8H_{46}	C_7H_{50}	C_6H_{52}	C_5H_{44}	C_4H_{46}	C_3H_{48}	$C_{24}H_{50}$	$C_{23}H_{52}$	$C_{22}H_{54}$	$C_{21}H_{56}$	$C_{20}H_{58}$	$C_{19}H_{60}$	$C_{18}H_{62}$	$C_{17}H_{64}$	$C_{16}H_{66}$	$C_{15}H_{68}$	$C_{14}H_{70}$	$C_{13}H_{72}$	$C_{12}H_{74}$
3	$C_{10}H_{34}$	C_9H_{38}	C_8H_{46}	C_7H_{50}	C_6H_{52}	C_5H_{44}	C_4H_{46}	C_3H_{48}	$C_{24}H_{50}$	$C_{23}H_{52}$	$C_{22}H_{54}$	$C_{21}H_{56}$	$C_{20}H_{58}$	$C_{19}H_{60}$	$C_{18}H_{62}$	$C_{17}H_{64}$	$C_{16}H_{66}$	$C_{15}H_{68}$	$C_{14}H_{70}$	$C_{13}H_{72}$	$C_{12}H_{74}$
4	$C_{10}H_{34}$	C_9H_{38}	C_8H_{46}	C_7H_{50}	C_6H_{52}	C_5H_{44}	C_4H_{46}	C_3H_{48}	$C_{24}H_{50}$	$C_{23}H_{52}$	$C_{22}H_{54}$	$C_{21}H_{56}$	$C_{20}H_{58}$	$C_{19}H_{60}$	$C_{18}H_{62}$	$C_{17}H_{64}$	$C_{16}H_{66}$	$C_{15}H_{68}$	$C_{14}H_{70}$	$C_{13}H_{72}$	$C_{12}H_{74}$
5	$C_{10}H_{34}$	C_9H_{38}	C_8H_{46}	C_7H_{50}	C_6H_{52}	C_5H_{44}	C_4H_{46}	C_3H_{48}	$C_{24}H_{50}$	$C_{23}H_{52}$	$C_{22}H_{54}$	$C_{21}H_{56}$	$C_{20}H_{58}$	$C_{19}H_{60}$	$C_{18}H_{62}$	$C_{17}H_{64}$	$C_{16}H_{66}$	$C_{15}H_{68}$	$C_{14}H_{70}$	$C_{13}H_{72}$	$C_{12}H_{74}$

Table I-S. Input modal composition mass fractions (by columns) in the nucleation mode and composition standard deviation for involatile core of 1%.

		modal composition																	
σ		$C_{10}H_{34}$	$C_{11}H_{36}$	$C_{18}H_{38}$	$C_{19}H_{40}$	$C_{20}H_{42}$	$C_{21}H_{44}$	$C_{22}H_{46}$	$C_{23}H_{48}$	$C_{24}H_{50}$	$C_{25}H_{52}$	$C_{26}H_{54}$	$C_{27}H_{56}$	$C_{28}H_{58}$	$C_{29}H_{60}$	$C_{30}H_{62}$	$C_{31}H_{64}$	$C_{32}H_{66}$	
1		5.42E-01	2.44E-01	5.15E-02	4.21E-03	1.27E-04	1.41E-06	5.77E-09	8.68E-12	4.80E-15	9.77E-19	7.31E-23	2.01E-27	2.04E-32	7.60E-38	1.05E-43	5.58E-50	1.39E-56	
		3.29E-01	4.03E-01	2.31E-01	5.13E-02	4.21E-03	1.27E-04	1.41E-06	5.77E-09	8.68E-12	4.80E-15	9.77E-19	7.31E-23	2.01E-27	2.04E-32	7.63E-38	1.11E-43	7.51E-50	
		7.33E-02	2.44E-01	3.81E-01	2.30E-01	5.13E-02	4.21E-03	1.27E-04	1.41E-06	5.77E-09	8.68E-12	4.80E-15	9.77E-19	7.31E-23	2.01E-27	2.05E-32	8.07E-38	1.49E-43	
		6.02E-03	5.45E-02	2.31E-01	3.79E-01	2.30E-01	5.13E-02	4.21E-03	1.27E-04	1.41E-06	5.77E-09	8.68E-12	4.80E-15	9.77E-19	7.31E-23	2.02E-27	2.17E-32	1.09E-37	
		1.82E-04	4.47E-03	5.15E-02	2.30E-01	3.79E-01	2.30E-01	5.13E-02	4.21E-03	1.27E-04	1.41E-06	5.77E-09	8.68E-12	4.80E-15	9.77E-19	7.34E-23	2.14E-27	2.92E-32	
		2.02E-06	1.35E-04	4.23E-03	5.13E-02	2.30E-01	3.79E-01	2.30E-01	5.13E-02	4.21E-03	1.27E-04	1.41E-06	5.77E-09	8.68E-12	4.80E-15	9.81E-19	7.76E-23	2.88E-27	
		8.25E-09	1.50E-06	1.28E-03	4.21E-03	5.13E-02	2.30E-01	3.79E-01	2.30E-01	5.13E-02	4.21E-03	1.27E-04	1.41E-06	5.77E-09	8.68E-12	4.82E-15	1.04E-18	1.05E-22	
		1.24E-11	6.13E-09	1.42E-06	1.27E-04	4.21E-03	5.13E-02	2.30E-01	3.79E-01	2.30E-01	5.13E-02	4.21E-03	1.27E-04	1.41E-06	5.77E-09	8.72E-12	5.10E-15	1.40E-18	
		6.86E-15	9.22E-12	5.80E-09	1.41E-06	1.27E-04	4.21E-03	5.13E-02	2.30E-01	3.79E-01	2.30E-01	5.13E-02	4.21E-03	1.27E-04	1.41E-06	5.80E-09	9.22E-12	6.86E-15	
		1.40E-18	5.10E-15	8.72E-12	5.77E-09	1.41E-06	1.27E-04	4.21E-03	5.13E-02	2.30E-01	3.79E-01	2.30E-01	5.13E-02	4.21E-03	1.27E-04	1.42E-06	6.13E-09	1.24E-11	
		1.05E-22	1.04E-15	4.82E-15	6.86E-12	5.77E-09	1.41E-06	1.27E-04	4.21E-03	5.13E-02	2.30E-01	3.79E-01	2.30E-01	5.13E-02	4.21E-03	1.28E-04	1.50E-06	8.25E-09	
		2.88E-27	7.76E-23	9.81E-19	4.80E-15	8.68E-12	5.77E-09	1.41E-06	1.27E-04	4.21E-03	5.13E-02	2.30E-01	3.79E-01	2.30E-01	5.13E-02	4.23E-03	1.35E-04	2.02E-06	
		2.92E-32	1.24E-27	7.34E-23	9.77E-19	4.80E-15	8.68E-12	5.77E-09	1.41E-06	1.27E-04	4.21E-03	5.13E-02	2.30E-01	3.79E-01	2.30E-01	5.15E-02	4.47E-03	1.82E-04	
		1.09E-37	2.17E-32	2.02E-27	7.31E-23	9.77E-19	4.80E-15	8.68E-12	5.77E-09	1.41E-06	1.27E-04	4.21E-03	5.13E-02	2.30E-01	3.79E-01	2.31E-01	5.45E-02	6.02E-03	
		1.49E-43	8.07E-38	2.05E-32	2.01E-27	7.31E-23	9.77E-19	4.80E-15	8.68E-12	5.77E-09	1.41E-06	1.27E-04	4.21E-03	5.13E-02	2.30E-01	3.81E-01	2.44E-01	7.33E-02	
		7.51E-50	1.11E-43	7.63E-38	2.04E-32	2.01E-27	7.31E-23	9.77E-19	4.80E-15	8.68E-12	5.77E-09	1.41E-06	1.27E-04	4.21E-03	5.13E-02	2.31E-01	4.03E-01	3.29E-01	
		1.39E-56	5.58E-50	1.05E-43	7.60E-38	2.04E-32	2.01E-27	7.31E-23	9.77E-19	4.80E-15	8.68E-12	5.77E-09	1.41E-06	1.27E-04	4.21E-03	5.15E-02	2.44E-01	5.42E-01	
2		3.16E-01	2.16E-01	1.28E-01	6.40E-02	2.59E-02	8.35E-03	2.11E-03	4.15E-04	6.36E-05	7.59E-06	7.07E-07	5.13E-08	2.92E-09	1.32E-10	4.84E-12	1.49E-13	4.00E-15	
		2.79E-09	2.44E-01	1.86E-01	1.20E-01	6.22E-02	2.57E-02	8.33E-03	2.11E-03	4.15E-04	6.36E-05	7.60E-06	7.08E-07	5.18E-08	3.00E-09	1.41E-10	5.59E-12	1.93E-13	
		1.92E-01	2.16E-01	2.11E-01	1.74E-01	1.61E-01	6.17E-02	2.57E-02	8.33E-03	2.11E-03	4.15E-04	6.36E-05	7.61E-06	7.14E-07	5.32E-08	3.22E-09	1.63E-10	7.23E-12	
		1.03E-01	1.48E-01	1.86E-01	1.97E-01	1.69E-01	1.51E-01	6.16E-02	2.56E-02	8.33E-03	2.11E-03	4.15E-04	6.37E-05	7.68E-06	7.34E-07	5.70E-08	3.72E-09	2.11E-10	
		4.28E-02	7.93E-02	1.28E-01	1.74E-01	1.92E-01	1.68E-01	1.51E-01	6.15E-02	2.56E-02	8.33E-03	2.11E-03	4.16E-04	6.43E-05	7.90E-06	7.87E-07	6.59E-08	4.81E-09	
		1.39E-02	3.31E-02	6.86E-02	1.20E-01	1.69E-01	1.90E-01	1.67E-01	1.51E-01	6.16E-02	2.56E-02	8.33E-03	2.11E-03	4.19E-04	6.61E-05	8.47E-06	9.10E-07	8.53E-08	
		6.91E-04	2.71E-03	9.28E-03	6.22E-02	6.22E-02	1.05E-01	1.67E-01	1.90E-01	1.67E-01	1.67E-01	1.90E-01	1.67E-01	1.67E-01	2.57E-02	8.35E-03	2.13E-04	7.09E-06	
		1.06E-04	5.34E-04	2.35E-03	8.66E-03	2.59E-02	6.17E-02	1.05E-01	1.67E-01	1.90E-01	1.67E-01	1.67E-01	1.90E-01	1.67E-01	2.59E-02	8.66E-03	2.35E-03	5.34E-04	
		1.27E-05	8.19E-05	4.62E-04	2.19E-03	8.48E-03	2.57E-02	6.16E-02	1.15E-01	1.67E-01	1.90E-01	1.67E-01	1.67E-01	1.90E-01	2.62E-02	8.42E-03	2.19E-03	4.61E-04	
		1.18E-06	9.79E-06	7.09E-05	4.31E-04	2.13E-03	8.35E-03	2.57E-02	6.15E-02	1.15E-01	1.67E-01	1.90E-01	1.67E-01	1.67E-01	2.62E-02	8.38E-03	2.17E-03	4.61E-04	
		8.53E-08	9.10E-07	8.47E-05	6.61E-05	4.19E-04	2.11E-03	8.33E-03	2.56E-02	6.15E-02	1.15E-01	1.67E-01	1.90E-01	1.67E-01	1.67E-01	2.62E-02	8.31E-03	2.13E-02	
		4.81E-09	6.59E-08	7.87E-07	7.90E-06	6.43E-05	4.16E-04	2.11E-03	8.33E-03	2.56E-02	6.15E-02	1.15E-01	1.67E-01	1.90E-01	1.67E-01	1.67E-01	2.62E-02	8.31E-03	2.13E-02
		7.23E-12	1.63E-10	3.22E-09	5.23E-08	7.14E-07	7.61E-06	6.36E-05	4.16E-05	2.11E-03	8.33E-03	2.57E-02	6.17E-02	1.16E-01	1.74E-01	2.11E-01	2.16E-01	1.92E-01	
		1.93E-13	5.59E-12	1.41E-10	3.00E-09	5.18E-08	7.08E-07	7.60E-06	6.36E-05	4.15E-04	2.11E-03	8.33E-03	2.57E-02	6.12E-02	1.20E-01	1.86E-01	2.44E-01	2.79E-01	
		4.00E-15	1.49E-13	8.48E-12	3.12E-10	2.92E-09	5.13E-08	7.07E-07	7.59E-06	6.36E-05	4.15E-04	2.11E-03	8.35E-03	2.59E-02	6.40E-02	1.28E-01	2.16E-01	3.16E-01	
3		2.23E-01	1.73E-01	8.71E-01	5.95E-02	3.26E-02	1.74E-02	8.36E-03	3.62E-03	4.14E-03	4.96E-04	1.57E-04	4.54E-05	1.20E-05	2.95E-06	6.80E-07	1.48E-07		
		2.11E-01	1.82E-01	1.50E-01	1.15E-01	8.20E-02	5.37E-02	3.20E-02	1.72E-02	8.34E-03	3.63E-03	4.12E-03	5.05E-04	1.63E-04	4.82E-05	1.32E-05	3.41E-06	8.31E-07	
		1.79E-01	1.73E-01	1.58E-01	1.36E-01	1.08E-01	7.92E-02	5.27E-02	3.17E-02	1.72E-02	8.36E-03	3.66E-03	4.15E-03	5.23E-04	1.73E-04	5.31E-05	1.53E-05	4.16E-06	
		1.35E-01	1.46E-01	1.50E-01	1.44E-01	1.28E-01	1.05E-01	7.78E-02	5.23E-02	3.16E-02	1.72E-02	8.37E-03	3.68E-03	4.16E-03	5.24E-04	1.74E-04	5.32E-05	1.54E-06	
		9.17E-02	1.11E-01	1.27E-01	1.36E-01	1.03E-01	1.24E-01	1.03E-01	7.71E-02	5.22E-02	3.17E-02	1.72E-02	8.39E-03	3.69E-03	4.17E-03	5.25E-04	1.75E-04	5.33E-05	
		5.56E-02	7.50E-02	1.15E-01	1.28E-01	1.28E-01	1.31E-01	1.21E-01	1.02E-01	7.70E-02	5.23E-02	3.20E-02	1.72E-02	8.40E-03	3.70E-03	4.18E-03	5.26E-04	1.76E-04	
		3.02E-02	4.55E-02	6.50E-02	8.71E-02	1.08E-01	1.24E-01	1.28E-01	1.20E-01	7.71E-02	5.27E-02	3.22E-02	1.73E-02	8.43E-03	3.72E-03	4.20E-03	5.27E-04	1.77E-04	
		1.47E-02	2.47E-02	3.94E-02	5.91E-02	8.32E-02	1.05E-01	1.21E-01	1.27E-01	1.20E-01	7.72E-02	5.28E-02	3.23E-02	1.74E-02	8.45E-03	3.73E-03	4.24E-03	5.28E-04	
		6.37E-04	2.03E-03	4.52E-03	9.44E-03	1.83E-02	3.26E-02	5.27E-02	7.71E-02	1.02E-01	1.28E-01	1.24E-01	1.20E-01	7.92E-02	5.35E-02	3.28E-02	4.55E-02	3.02E-02	
		2.68E-04	7.05E-04	1.76E-03	4.10E-03	8.89E-03	1.77E-02	3.20E-02	5.23E-02	7.70E-02	1.02E-01	1.28E-01	1.24E-01	1.20E-01	7.95E-02	5.36E-02	3.29E-02	4.56E-02	
		7.48E-05	2.20E-04	6.11E-04	1.60E-03	3.86E-03	8.59E-03	1.74E-02	3.17E-02	5.22E-02	7.71E-02	1.03E-01	1.28E-01	1.25E-01	1.20E-01	7.97E-02	5.37E-02	3.30E-02	
		1.87E-05	6.12E-05	1.90E-04	5.55E-04	1.													

modal composition																	
σ	$C_{18}H_{34}$	$C_{17}H_{35}$	$C_{19}H_{38}$	$C_{19}H_{40}$	$C_{20}H_{42}$	$C_{21}H_{44}$	$C_{22}H_{46}$	$C_{22}H_{48}$	$C_{23}H_{50}$	$C_{24}H_{52}$	$C_{24}H_{54}$	$C_{25}H_{56}$	$C_{26}H_{58}$	$C_{26}H_{60}$	$C_{27}H_{62}$	$C_{27}H_{64}$	
1	5.13E-01	2.31E-01	4.88E-02	3.99E-03	1.20E-04	1.34E-06	5.47E-09	8.22E-12	4.55E-15	9.25E-19	6.93E-23	1.91E-27	1.93E-32	7.20E-38	9.91E-44	5.29E-50	1.32E-56
	3.11E-01	3.81E-01	2.19E-01	4.86E-02	3.69E-03	1.20E-04	1.34E-06	5.47E-09	8.22E-12	4.55E-15	9.25E-19	6.93E-23	1.91E-27	1.93E-32	7.23E-38	1.05E-43	7.12E-50
	6.95E-02	2.31E-01	3.61E-01	2.18E-01	4.86E-02	3.99E-03	1.20E-04	1.34E-06	5.47E-09	8.22E-12	4.55E-15	9.25E-19	6.93E-23	1.91E-27	1.94E-32	7.65E-38	1.41E-43
	5.70E-03	5.16E-02	2.19E-01	3.59E-01	2.18E-01	4.86E-02	3.99E-03	1.20E-04	1.34E-06	5.47E-09	8.22E-12	4.55E-15	9.25E-19	6.93E-23	1.92E-27	2.05E-32	1.03E-37
	1.72E-04	4.24E-03	4.88E-02	2.18E-01	3.59E-01	2.18E-01	4.86E-02	3.99E-03	1.20E-04	1.34E-06	5.47E-09	8.22E-12	4.55E-15	9.25E-19	6.96E-23	2.03E-27	2.76E-32
	1.91E-06	1.28E-04	4.01E-03	4.86E-02	2.18E-01	3.59E-01	2.18E-01	4.86E-02	3.99E-03	1.20E-04	1.34E-06	5.47E-09	8.22E-12	4.55E-15	9.25E-19	7.36E-23	2.73E-27
	7.82E-09	1.42E-06	1.21E-01	3.99E-03	4.86E-02	2.18E-01	3.59E-01	2.18E-01	4.86E-02	3.99E-03	1.20E-04	1.34E-06	5.47E-09	8.22E-12	4.57E-15	9.83E-19	9.90E-23
	1.18E-11	5.81E-09	1.34E-04	1.20E-04	3.99E-04	4.86E-02	2.18E-01	3.59E-01	2.18E-01	4.86E-02	3.99E-03	1.20E-04	1.34E-06	5.47E-09	8.26E-12	4.83E-15	1.32E-18
	6.50E-15	8.73E-12	5.49E-02	1.34E-04	1.20E-04	3.99E-03	4.86E-02	2.18E-01	3.59E-01	2.18E-01	4.86E-02	3.99E-03	1.20E-04	1.34E-06	5.49E-09	8.73E-12	6.50E-15
	1.32E-15	4.83E-15	8.26E-12	5.47E-09	1.34E-06	1.20E-04	3.99E-03	4.86E-02	2.18E-01	3.59E-01	2.18E-01	4.86E-02	3.99E-03	1.20E-04	1.34E-06	5.81E-09	1.18E-11
	9.90E-23	9.83E-19	4.57E-15	8.22E-12	5.47E-09	1.34E-06	1.20E-04	3.99E-03	4.86E-02	2.18E-01	3.59E-01	2.18E-01	4.86E-02	3.99E-03	1.21E-04	1.42E-06	7.82E-09
	2.73E-27	7.36E-23	9.29E-19	4.55E-15	8.22E-12	5.47E-09	1.34E-06	1.20E-04	3.99E-03	4.86E-02	2.18E-01	3.59E-01	2.18E-01	4.86E-02	4.01E-03	1.28E-04	1.91E-06
	2.76E-32	2.03E-27	6.96E-23	9.25E-19	4.55E-15	8.22E-12	5.47E-09	1.34E-06	1.20E-04	3.99E-03	4.86E-02	2.18E-01	3.59E-01	2.18E-01	4.86E-02	4.24E-03	1.72E-04
	1.03E-33	2.05E-32	1.92E-27	6.93E-23	9.25E-19	4.55E-15	8.22E-12	5.47E-09	1.34E-06	1.20E-04	3.99E-03	4.86E-02	2.18E-01	3.61E-01	2.31E-01	6.95E-02	5.70E-03
	7.12E-50	1.05E-43	7.23E-38	1.93E-32	1.91E-27	6.93E-23	9.25E-19	4.55E-15	8.22E-12	5.47E-09	1.34E-06	1.20E-04	3.99E-03	4.86E-02	2.19E-01	3.81E-01	3.11E-01
	1.32E-56	5.29E-50	9.91E-44	7.20E-38	9.91E-44	5.29E-50	1.32E-56	5.29E-50	9.91E-44	5.29E-50	1.32E-56	5.29E-50	9.91E-44	5.29E-50	1.32E-56	5.29E-50	1.32E-56
2	$C_{18}H_{34}$	$C_{17}H_{35}$	$C_{19}H_{38}$	$C_{19}H_{40}$	$C_{20}H_{42}$	$C_{21}H_{44}$	$C_{22}H_{46}$	$C_{22}H_{48}$	$C_{23}H_{50}$	$C_{24}H_{52}$	$C_{24}H_{54}$	$C_{25}H_{56}$	$C_{26}H_{58}$	$C_{26}H_{60}$	$C_{27}H_{62}$	$C_{27}H_{64}$	
	2.99E-01	2.04E-01	1.21E-01	6.06E-02	2.46E-02	7.91E-03	2.00E-03	3.93E-04	6.02E-05	7.19E-06	6.69E-07	4.86E-08	2.77E-09	1.25E-10	4.58E-12	1.41E-13	3.79E-15
	2.64E-01	2.31E-01	1.77E-01	1.13E-01	5.90E-02	2.44E-02	7.89E-03	1.99E-03	3.93E-04	6.02E-05	7.20E-06	6.71E-07	4.90E-08	2.84E-09	1.34E-10	5.30E-12	1.83E-13
	1.82E-01	2.04E-01	2.00E-01	1.65E-01	1.10E-01	5.84E-02	2.43E-02	7.89E-03	1.99E-03	3.93E-04	6.03E-05	7.21E-06	6.77E-07	5.04E-08	3.05E-09	1.55E-10	6.85E-12
	9.72E-02	1.40E-01	1.77E-01	1.87E-01	1.60E-01	1.09E-01	5.83E-02	2.43E-02	7.89E-03	1.99E-03	3.93E-04	6.04E-05	7.28E-06	6.96E-07	5.40E-08	3.52E-09	2.00E-10
	4.05E-02	7.51E-02	1.21E-01	1.65E-01	1.82E-01	1.59E-01	1.09E-01	5.83E-02	2.43E-02	7.89E-03	2.00E-03	3.94E-04	6.05E-05	7.48E-06	7.46E-07	6.25E-08	4.56E-09
	1.32E-02	3.13E-02	6.50E-02	1.12E-01	1.60E-01	1.80E-01	1.59E-01	1.09E-01	5.83E-02	2.43E-02	7.89E-03	2.00E-03	3.94E-04	6.05E-05	8.20E-06	8.62E-07	8.08E-08
	3.33E-03	1.02E-02	2.71E-02	6.06E-02	1.10E-01	1.59E-01	1.80E-01	1.58E-01	1.09E-01	5.83E-02	2.43E-02	7.91E-03	2.02E-03	4.08E-04	6.72E-05	9.27E-06	1.12E-06
	6.55E-04	2.57E-03	8.80E-03	2.53E-02	5.90E-02	1.09E-01	1.59E-01	1.80E-01	1.58E-01	1.09E-01	5.83E-02	2.44E-02	7.98E-03	2.07E-03	4.38E-04	7.76E-05	1.20E-05
	1.00E-04	5.06E-04	2.22E-03	8.20E-03	2.46E-02	5.84E-02	1.09E-01	1.58E-01	1.80E-01	1.58E-01	1.09E-01	5.84E-02	2.46E-02	8.20E-03	2.22E-03	5.06E-04	1.00E-04
	1.20E-05	7.76E-05	4.38E-04	2.07E-03	7.98E-03	2.44E-02	5.83E-02	1.09E-01	1.58E-01	1.80E-01	1.58E-01	1.09E-01	5.90E-02	2.53E-02	8.80E-03	2.57E-03	6.55E-04
	1.12E-06	9.27E-06	6.72E-05	4.08E-04	2.02E-03	7.91E-03	2.43E-02	5.83E-02	1.09E-01	1.58E-01	1.80E-01	1.58E-01	1.09E-01	6.06E-02	2.71E-02	1.02E-02	3.33E-03
	8.08E-08	8.62E-07	8.02E-05	6.26E-05	3.97E-04	2.00E-03	7.89E-03	2.43E-02	5.83E-02	1.09E-01	1.59E-01	1.80E-01	1.60E-01	1.13E-01	6.50E-02	3.13E-02	1.32E-02
	4.56E-09	6.25E-08	7.46E-07	7.48E-06	6.09E-05	3.94E-04	2.00E-03	7.89E-03	2.43E-02	5.83E-02	1.09E-01	1.59E-01	1.80E-01	1.60E-01	1.13E-01	6.50E-02	4.05E-02
	2.00E-10	3.52E-09	5.40E-08	6.96E-07	7.28E-06	6.04E-05	3.93E-04	2.00E-03	7.89E-03	2.43E-02	5.83E-02	1.09E-01	1.59E-01	1.80E-01	1.60E-01	1.13E-01	9.72E-02
	6.85E-12	1.55E-10	3.05E-09	5.04E-08	6.77E-07	7.21E-06	6.03E-05	3.93E-04	1.99E-03	7.89E-03	2.43E-02	5.84E-02	1.10E-01	1.65E-01	2.00E-01	1.82E-01	1.38E-01
	1.83E-13	5.30E-12	1.34E-10	2.84E-09	4.90E-08	6.71E-07	7.20E-06	6.02E-05	3.93E-04	1.99E-03	7.89E-03	2.44E-02	5.90E-02	1.13E-01	1.77E-01	2.31E-01	2.64E-01
	3.79E-15	1.41E-13	4.58E-12	1.25E-10	2.77E-09	4.86E-08	6.69E-07	7.19E-06	6.02E-05	3.93E-04	2.00E-03	7.91E-03	2.46E-02	6.06E-02	1.21E-01	2.04E-01	2.99E-01
3	$C_{16}H_{34}$	$C_{17}H_{36}$	$C_{18}H_{38}$	$C_{19}H_{40}$	$C_{20}H_{42}$	$C_{21}H_{44}$	$C_{22}H_{46}$	$C_{23}H_{48}$	$C_{24}H_{50}$	$C_{25}H_{52}$	$C_{26}H_{54}$	$C_{27}H_{56}$	$C_{28}H_{58}$	$C_{29}H_{60}$	$C_{30}H_{62}$	$C_{31}H_{64}$	$C_{32}H_{66}$
	2.11E-01	1.64E-01	1.20E-01	8.25E-02	5.27E-02	3.09E-02	1.64E-02	7.92E-03	3.43E-03	1.34E-03	4.70E-04	1.49E-04	4.30E-05	1.14E-05	2.80E-06	6.44E-07	1.41E-07
	2.00E-01	1.73E-01	1.42E-01	1.09E-01	7.77E-02	5.09E-02	3.03E-02	1.63E-02	7.90E-03	3.44E-03	1.35E-03	4.78E-04	1.54E-04	4.57E-05	1.25E-05	3.23E-06	7.87E-07
	1.69E-01	1.64E-01	1.50E-01	1.29E-01	1.03E-01	7.51E-02	5.00E-02	3.00E-02	1.63E-02	7.92E-03	3.47E-03	1.37E-03	4.95E-04	1.64E-04	5.03E-05	1.45E-05	3.94E-06
	8.69E-02	1.05E-01	1.20E-01	1.29E-01	1.03E-01	7.48E-02	5.00E-02	3.00E-02	1.64E-02	7.93E-03	3.48E-03	1.38E-03	4.96E-04	1.65E-04	5.04E-05	1.47E-05	3.95E-06
	5.27E-02	1.11E-01	1.09E-01	1.21E-01	1.02E-01	7.47E-02	5.00E-02	3.00E-02	1.65E-02	7.94E-03	3.49E-03	1.39E-03	4.97E-04	1.66E-04	5.05E-05	1.48E-05	3.96E-06
	1.39E-01	2.34E-02	3.74E-02	5.59E-02	7.77E-02	9.91E-02	1.15E-01	1.20E-01	1.41E-01	9.65E-02	7.37E-02	5.09E-02	3.19E-02	1.84E-02	9.85E-03	4.94E-03	2.35E-03
	6.04E-03	1.14E-02	2.03E-02	3.39E-02	5.27E-02	7.51E-02	9.73E-02	1.14E-01	1.20E-01	1.41E-01	9.73E-02	7.51E-02	5.27E-02	3.39E-02	2.03E-02	1.14E-02	6.04E-03
	2.35E-03	4.94E-03	9.85E-03	1.84E-02	3.19E-02	5.09E-02	7.37E-02	9.65E-02	1.14E-01	1.20E-01	1.41E-01	9.91E-02	7.77E-02	5.59E-02	3.47E-02	2.34E-02	1.39E-02
	8.17E-04	1.92E-03	4.28E-03	8.95E-03	1.73E-02	3.09E-02	5.00E-02	7.31E-02	9.63E-02	1.14E-01	1.22E-01	1.42E-01	1.17E-01	8.25E-02	6.17E-		

σ	modal composition																		
1	$C_{10}H_{34}$	$C_{11}H_{35}$	$C_{12}H_{38}$	$C_{13}H_{40}$	$C_{20}H_{42}$	$C_{21}H_{44}$	$C_{22}H_{46}$	$C_{23}H_{48}$	$C_{24}H_{50}$	$C_{25}H_{52}$	$C_{26}H_{54}$	$C_{27}H_{56}$	$C_{28}H_{58}$	$C_{29}H_{60}$	$C_{30}H_{62}$	$C_{31}H_{64}$	$C_{32}H_{66}$		
	5.70E-02	2.57E-02	5.42E-03	4.43E-04	1.34E-05	1.49E-07	6.08E-10	9.13E-13	5.05E-16	1.03E-19	7.69E-24	2.12E-28	2.15E-33	8.00E-39	1.10E-44	5.87E-51	1.47E-57		
	3.46E-02	4.24E-02	2.43E-02	5.40E-03	4.43E-04	1.34E-05	1.49E-07	6.08E-10	9.13E-13	5.05E-16	1.03E-19	7.69E-24	2.12E-28	2.15E-33	8.04E-39	1.16E-44	7.91E-51		
	7.72E-03	2.57E-02	4.01E-02	2.42E-02	5.40E-03	4.43E-04	1.34E-05	1.49E-07	6.08E-10	9.13E-13	5.05E-16	1.03E-19	7.69E-24	2.12E-28	2.16E-33	8.50E-39	1.57E-44		
	6.34E-04	5.73E-03	2.43E-02	3.99E-02	2.42E-02	5.40E-03	4.43E-04	1.34E-05	1.49E-07	6.08E-10	9.13E-13	5.05E-16	1.03E-19	7.70E-24	2.13E-28	2.28E-33	1.14E-38		
	1.91E-05	4.71E-04	5.42E-03	2.42E-02	3.99E-02	2.42E-02	5.40E-03	4.43E-04	1.34E-05	1.49E-07	6.08E-10	9.13E-13	5.05E-16	1.03E-19	7.73E-24	2.25E-28	3.07E-33		
	2.13E-07	1.42E-05	4.45E-04	5.40E-03	2.42E-02	3.99E-02	2.42E-02	5.40E-03	4.43E-04	1.34E-05	1.49E-07	6.08E-10	9.13E-13	5.05E-16	1.03E-19	8.17E-24	3.03E-28		
	8.69E-10	1.58E-07	1.34E-05	4.43E-04	5.40E-03	2.42E-02	3.99E-02	2.42E-02	5.40E-03	4.43E-04	1.34E-05	1.49E-07	6.08E-10	9.14E-13	5.08E-16	1.09E-19	1.10E-23		
	1.31E-12	6.45E-10	1.49E-07	1.34E-05	4.43E-04	5.40E-03	2.42E-02	3.99E-02	2.42E-02	5.40E-03	4.43E-04	1.34E-05	1.49E-07	6.08E-10	9.18E-13	5.37E-16	1.47E-19		
	7.22E-16	9.70E-13	6.10E-10	1.49E-07	1.34E-05	4.43E-04	5.40E-03	2.42E-02	3.99E-02	2.42E-02	5.40E-03	4.43E-04	1.34E-05	1.49E-07	6.10E-10	9.70E-13	7.22E-16		
	1.47E-19	5.37E-16	9.18E-13	6.08E-10	1.49E-07	1.34E-05	4.43E-04	5.40E-03	2.42E-02	3.99E-02	2.42E-02	5.40E-03	4.43E-04	1.34E-05	1.49E-07	6.45E-10	1.31E-12		
	1.10E-23	1.09E-19	5.08E-16	9.14E-13	6.08E-10	1.49E-07	1.34E-05	4.43E-04	5.40E-03	2.42E-02	3.99E-02	2.42E-02	5.40E-03	4.43E-04	1.34E-05	1.58E-07	8.69E-10		
	3.03E-28	8.17E-24	1.03E-19	5.05E-16	9.13E-13	6.08E-10	1.49E-07	1.34E-05	4.43E-04	5.40E-03	2.42E-02	3.99E-02	2.42E-02	5.40E-03	4.45E-04	1.42E-05	2.13E-07		
	3.07E-33	2.25E-28	7.73E-24	1.03E-19	5.05E-16	9.13E-13	6.08E-10	1.49E-07	1.34E-05	4.43E-04	5.40E-03	2.42E-02	3.99E-02	2.42E-02	5.42E-03	4.71E-04	1.91E-05		
	1.14E-38	2.28E-33	2.13E-28	7.70E-24	1.03E-19	5.05E-16	9.13E-13	6.08E-10	1.49E-07	1.34E-05	4.43E-04	5.40E-03	2.42E-02	3.99E-02	2.43E-02	5.73E-03	6.34E-04		
	1.57E-44	8.50E-39	2.16E-33	2.12E-28	7.69E-24	1.03E-19	5.05E-16	9.13E-13	6.08E-10	1.49E-07	1.34E-05	4.43E-04	5.40E-03	2.43E-02	4.24E-02	3.46E-02	7.72E-03		
	7.91E-51	1.16E-44	8.04E-39	2.15E-33	2.12E-28	7.69E-24	1.03E-19	5.05E-16	9.13E-13	6.08E-10	1.49E-07	1.34E-05	4.43E-04	5.40E-03	2.43E-02	4.24E-02	5.70E-02		
	1.47E-57	5.87E-51	1.10E-44	8.00E-39	2.15E-33	2.12E-28	7.69E-24	1.03E-19	5.05E-16	9.13E-13	6.08E-10	1.49E-07	1.34E-05	4.43E-04	5.42E-03	2.57E-02	5.70E-02		
2	$C_{10}H_{34}$	$C_{11}H_{35}$	$C_{12}H_{38}$	$C_{13}H_{40}$	$C_{20}H_{42}$	$C_{21}H_{44}$	$C_{22}H_{46}$	$C_{23}H_{48}$	$C_{24}H_{50}$	$C_{25}H_{52}$	$C_{26}H_{54}$	$C_{27}H_{56}$	$C_{28}H_{58}$	$C_{29}H_{60}$	$C_{30}H_{62}$	$C_{31}H_{64}$	$C_{32}H_{66}$		
	3.33E-02	2.27E-02	1.35E-02	6.74E-03	2.73E-03	8.79E-04	2.22E-04	4.36E-05	6.69E-06	7.99E-07	7.44E-08	5.40E-09	3.07E-10	1.39E-11	5.09E-13	1.57E-14	4.21E-14		
	2.94E-02	2.57E-02	1.96E-02	1.26E-02	6.55E-03	2.71E-03	8.77E-04	2.22E-04	4.36E-05	6.69E-06	8.00E-07	7.45E-08	5.45E-09	3.16E-10	1.49E-11	5.89E-13	2.03E-14		
	2.02E-02	2.27E-02	2.22E-02	1.83E-02	1.21E-02	6.49E-03	2.70E-03	8.76E-04	2.22E-04	4.36E-05	6.69E-06	8.01E-07	7.52E-08	5.60E-09	3.39E-10	1.72E-11	7.62E-13		
	1.08E-02	1.56E-02	2.07E-02	1.78E-02	1.21E-02	6.48E-03	2.70E-03	8.76E-04	2.22E-04	4.37E-05	6.71E-06	8.08E-07	7.73E-08	6.00E-09	3.92E-10	2.23E-11			
	4.50E-03	8.35E-03	1.35E-02	1.83E-02	2.02E-02	1.77E-02	1.21E-02	6.48E-03	2.70E-03	8.76E-04	2.22E-04	4.38E-05	6.77E-06	8.31E-07	8.29E-08	6.94E-09	5.07E-10		
	1.46E-03	3.48E-03	7.22E-03	1.26E-02	1.78E-02	2.00E-02	1.76E-02	1.21E-02	6.48E-03	2.70E-03	8.77E-04	2.22E-04	4.41E-05	6.96E-06	8.91E-07	9.58E-08	8.98E-09		
	3.69E-04	1.13E-03	3.01E-03	6.74E-03	1.22E-02	1.77E-02	2.00E-02	1.76E-02	1.21E-02	6.48E-03	2.70E-03	8.79E-04	2.24E-04	4.54E-05	7.46E-06	1.03E-06	1.24E-07		
	7.28E-05	2.86E-04	9.77E-04	2.81E-03	6.55E-03	1.21E-02	1.76E-02	1.99E-02	1.76E-02	1.21E-02	6.48E-03	2.71E-03	8.87E-04	2.30E-04	4.87E-05	8.63E-06	1.33E-06		
	1.12E-05	5.62E-05	2.47E-04	9.11E-04	2.73E-03	6.49E-03	1.21E-02	1.76E-02	1.99E-02	1.76E-02	1.21E-02	6.49E-03	2.73E-03	9.11E-04	2.47E-04	5.62E-05	1.12E-05		
	1.33E-06	8.63E-06	4.87E-05	2.30E-04	8.87E-04	2.71E-03	6.48E-03	1.21E-02	1.76E-02	1.99E-02	1.76E-02	1.21E-02	6.50E-03	2.81E-03	9.77E-04	2.86E-04	7.28E-05		
	1.24E-07	1.03E-06	7.46E-06	4.54E-05	2.24E-04	8.79E-04	2.70E-03	6.48E-03	1.21E-02	1.76E-02	1.99E-02	1.76E-02	1.21E-02	6.52E-03	2.82E-03	9.77E-04	2.86E-04	7.28E-05	
	8.98E-09	9.58E-09	8.91E-07	2.22E-04	8.77E-04	2.70E-03	6.48E-03	1.21E-02	1.76E-02	1.99E-02	1.76E-02	1.21E-02	6.53E-03	2.82E-03	9.77E-04	2.86E-04	7.28E-05		
	5.07E-10	6.94E-09	8.29E-08	8.31E-07	6.77E-06	4.38E-05	2.22E-04	8.76E-04	2.70E-03	6.48E-03	1.21E-02	1.76E-02	1.99E-02	1.76E-02	1.21E-02	6.54E-03	2.83E-03	9.45E-03	
	2.23E-11	3.92E-10	6.00E-09	7.73E-08	8.08E-07	6.71E-05	4.37E-05	2.22E-04	8.76E-04	2.70E-03	6.48E-03	1.21E-02	1.76E-02	1.99E-02	1.76E-02	1.21E-02	6.55E-03	2.84E-03	9.46E-03
	7.62E-13	1.72E-11	3.39E-10	5.60E-09	7.52E-08	8.01E-07	6.69E-06	4.36E-05	2.22E-04	8.76E-04	2.70E-03	6.49E-03	1.22E-02	1.76E-02	1.99E-02	1.76E-02	1.22E-02	6.56E-03	2.84E-03
	2.03E-14	5.89E-13	1.16E-11	3.16E-10	5.45E-09	7.45E-08	8.00E-07	6.69E-06	4.36E-05	2.22E-04	8.77E-04	2.71E-03	6.55E-03	1.22E-02	1.76E-02	1.99E-02	1.76E-02	1.22E-02	2.94E-02
	4.21E-16	1.57E-14	5.09E-13	3.07E-10	5.16E-09	7.44E-08	7.99E-07	6.69E-06	4.36E-05	2.22E-04	8.78E-04	2.73E-03	6.74E-03	1.23E-02	1.76E-02	1.99E-02	1.76E-02	1.23E-02	2.73E-02
3	$C_{10}H_{34}$	$C_{17}H_{36}$	$C_{18}H_{38}$	$C_{19}H_{40}$	$C_{20}H_{42}$	$C_{21}H_{44}$	$C_{22}H_{46}$	$C_{23}H_{48}$	$C_{24}H_{50}$	$C_{25}H_{52}$	$C_{26}H_{54}$	$C_{27}H_{56}$	$C_{28}H_{58}$	$C_{29}H_{60}$	$C_{30}H_{62}$	$C_{31}H_{64}$	$C_{32}H_{66}$		
	2.35E-02	1.82E-02	1.33E-02	9.17E-03	5.85E-03	3.43E-03	1.83E-03	8.80E-04	3.82E-04	1.49E-05	5.22E-05	1.66E-05	4.78E-06	1.26E-06	3.11E-07	7.16E-08	1.56E-08		
	2.22E-02	1.92E-02	1.57E-02	8.63E-03	5.65E-03	3.37E-03	1.81E-03	8.78E-04	3.82E-04	1.50E-05	5.32E-05	1.71E-05	5.07E-06	1.39E-06	3.59E-07	8.75E-08	1.57E-08		
	1.88E-02	1.82E-02	1.66E-02	1.43E-02	8.34E-03	5.55E-03	3.34E-03	1.81E-03	8.80E-04	3.86E-04	1.53E-05	5.50E-05	1.82E-05	5.58E-06	1.61E-06	4.38E-07			
	1.42E-02	1.54E-02	1.57E-02	1.51E-02	1.35E-02	8.19E-03	5.50E-03	3.33E-03	1.81E-03	8.87E-04	3.93E-04	1.58E-05	5.85E-05	2.00E-05	6.44E-06	1.96E-06			
	9.65E-03	1.17E-02	1.33E-02	1.42E-02	1.30E-02	8.08E-03	5.45E-03	3.34E-03	1.83E-03	9.04E-04	4.07E-04	1.68E-04	6.44E-05	2.31E-05	7.87E-06				
	5.85E-03	7.90E-03	1.01E-02	1.21E-02	1.35E-02	8.17E-03	5.35E-03	3.37E-03	1.82E-03	9.06E-04	4.13E-04	1.73E-04	6.45E-05	2.38E-05	7.83E-06				
	3.18E-03	4.79E-03	6.84E-03	9.17E-03	1.14E-02	1.30E-02	1.35E-02	1.27E-02	1.07E-02	8.12E-03	5.50E-03	3.37E-03	1.86E-03	9.36E-04	4.32E-04	1.85E-04	7.43E-05		
	1.54E-03	2.60E-03	4.15E-03	6.22E-03	8.63E-03	1.10E-02	1.28E-02	1.34E-02	1.26E-02	1.07E-02	8.13E-03	5.55E-03	3.43E-03	1.93E-03	9.49E-0				

n-alkanes $C_nH_{(2n+2)}$	Chickos&Lipkind 2008	EPI Suite	A) Nannoolal et al 2008			B) Myrdal and Yalkowsky 1997			Co) Compernolle et al 2011 for all boiling points	
			boiling point			boiling point				
			a	b	c	a	b	c		
n										
16		9.29E-001	2.87E-001	6.63E-001	5.38E-001	1.39E-001	3.46E-001	2.75E-001	3.05E-001	
17		4.32E-001	6.85E-002	2.45E-001	2.06E-001	3.14E-002	1.24E-001	1.03E-001	9.98E-002	
18		1.95E-001	1.54E-002	9.22E-002	7.91E-002	6.74E-003	4.55E-002	3.86E-002	3.27E-002	
19		8.97E-002	3.23E-003	3.54E-002	3.04E-002	1.38E-003	1.73E-002	1.47E-002	1.07E-002	
20		4.13E-002	6.33E-004	1.39E-002	1.17E-002	2.70E-004	6.76E-003	5.61E-003	3.50E-003	
21	6.93E-004	1.89E-002	1.16E-004	5.60E-003	4.47E-003	5.03E-005	2.73E-003	2.16E-003	1.15E-003	
22	2.09E-004	9.23E-003	1.97E-005	2.26E-003	1.71E-003	8.94E-006	1.11E-003	8.35E-004	3.75E-004	
23	6.95E-005	4.73E-003	3.10E-006	8.86E-004	6.52E-004	1.52E-006	4.45E-004	3.25E-004	1.23E-004	
24	2.31E-005	2.26E-003	4.50E-007	3.39E-004	2.48E-004	2.46E-007	1.75E-004	1.27E-004	4.01E-005	
25	8.51E-006	1.28E-002	6.01E-008	1.26E-004	9.38E-005	3.81E-008	6.71E-005	4.97E-005	1.31E-005	
26	2.83E-006	7.02E-004	7.37E-009	4.58E-005	3.53E-005	5.64E-009	2.53E-005	1.95E-005	4.30E-006	
27	1.15E-006	1.31E-004	8.25E-010	1.61E-005	1.32E-005	7.97E-010	9.36E-006	7.68E-006	1.41E-006	
28	3.14E-007	2.06E-004	8.40E-011	5.53E-006	4.94E-006	1.08E-010	3.39E-006	3.03E-006	4.61E-007	
29	1.05E-007	1.27E-004	7.74E-012	1.84E-006	1.83E-006	1.39E-011	1.20E-006	1.20E-006	1.51E-007	
30	3.48E-008	7.49E-005	6.44E-013	5.96E-007	6.75E-007	1.72E-012	4.20E-007	4.74E-007	4.93E-008	
31	1.16E-008	4.54E-005	4.81E-014	1.87E-007	2.47E-007	2.03E-013	1.43E-007	1.88E-007	1.61E-008	
32	3.49E-009	2.66E-005	3.20E-015	5.70E-008	9.01E-008	2.29E-014	4.80E-008	7.43E-008	5.28E-009	

Table 5-S. Vapour pressure data at 298 K from different sources corresponding to Figure 2 in the main manuscript. a, b, and c refer to the boiling point of Joback and Reid (1987), Stein and Brown (1994) and Nannoolal et al. (2004), respectively. A-a, B-c and Co are used in this study.

compound	vapour
C ₁₆ H ₃₄	6.42 (3.62)
C ₁₇ H ₃₆	9.32 (4.31)
C ₁₈ H ₃₈	9.36 (4.41)
C ₁₉ H ₄₀	9.74 (4.09)
C ₂₀ H ₄₂	8.35 (3.59)
C ₂₁ H ₄₄	6.20 (3.06)
C ₂₂ H ₄₆	3.97 (1.98)
C ₂₃ H ₄₈	2.32 (1.25)
C ₂₄ H ₅₀	1.59 (1.79)
C ₂₅ H ₅₂	1.20 (0.52)
C ₂₆ H ₅₄	1.00 (0.50)
C ₂₇ H ₅₆	1.28 (0.53)
C ₂₈ H ₅₈	1.03 (0.53)
C ₂₉ H ₆₀	1.24 (0.53)
C ₃₀ H ₆₂	0.80 (0.38)
C ₃₁ H ₆₄	0.77 (0.30)
C ₃₂ H ₆₆	0.42 (0.18)

260 *Table 6-S. Gas-phase concentrations used in the model. Numbers in parenthesis show the standard*
 261 *deviation of the measurements. Unit, ng m⁻³.*